1D laterally constrained inversion of 2D MT data

Daniela Costa Melo (UFPA) and Cícero Roberto Teixeira Régis (UFPA, INCT-GP)

This paper was prepared for presentation during the 15th International Congress of the Brazilian Geophysical Society, held in Rio de Janeiro, Brazil, 31 July to 3 August 2017.

Abstract

Applying 1D inversion to 2D magnetotelluric data allows the geophysicist to obtain fast and meaningful results, despite the inherent limitation of trying to approximate the subsurface response by models that vary only in one direction. This paper presents a way to minimize this limitation by performing the inversion of a set of MT soundings with constraints that take into account the lateral variations in the resistivity of the subsurface. The data from all sounding stations in a MT survey line are inverted jointly, producing layered columns with lateral smooth transitions. This process takes advantage of the low computational cost of 1D inversions, and it generates an approximate 2D model that can be useful as a first guess in a full 2D inversion. A synthetic example was used to evaluate the practical utility of the algorithm. The best results were obtained where the electrical structure of the earth is predominantly 1D and the structures showing 2D behaviour are not too close to each other.

Introduction

The interpretation of magnetotelluric (MT) data can be done either qualitatively, by means of the apparent resistivity an phase pseudo-sections, or by solving the inverse problem, which consists in determining the geo-electrical structures from the geophysical data. Starting with the observed data and a physical law, it is possible to obtain the parameters of an interpretive model of the subsurface. However, this is a difficult problem because of the complexity of the Earth's interior structures and the lack of enough information in the observed data to resolve those structures.

1D inversion of data from a single sounding station can be performed to resolve the resistivities of a layered interpretive model composed by a number of homogeneous layers over a homogeneous half-space. In this case, the forward modeling problem is a fast and accurate implementation of an analytical solution (Vozoff, 2012), which leads to an inversion program that is fast and economical in terms of memory requirement.

When lateral variations exist in the geo-electrical structure, a full 2D or even 3D inversion may be required for better accuracy. In these cases, one can simply start with a homogeneous interpretive model and leave the iterations converge to a solution. The choice of a first guess that may already be an approximation of the true values sought in the inversion can reduce the processing time by requiring less iterations to converge.

In this paper, we apply a method to generate approximate first models for MT inversion, using 1D joint inversion of data from the whole set of sounding stations spread on a survey line. The method implements a 1D laterally constrained inversion (LCI) technique (Miorelli, 2011) that is capable of performing inversion of large datasets, at a low computational cost. An analysis of the method is performed by applying it to synthetic data sets from two-dimensional models.

Methodology

1D inversion of data from a single MT sounding station can be performed to generate resistivity values for a sequence of homogeneous layers. This is an intrinsically ill-posed problem (Hadamard, 1902), due to the limited amount of information in the data, the existence of several different sources of noise, and the complexity of the real geological structures, which is always greater than that of the interpretive model. Therefore, a stable solution will be achieved only with the inclusion of some kind of constraint on the parameters. Usually, smoothing constraints (Constable et al., 1987) are used because they are simple to implement, and guarantee a solution, even if sometimes at the expense of a better fitting of the data.

Inverting each sounding separately can generate useful models. However, in most areas of interest there will be regions where the two-dimensional nature of the geo-electrical structures imposes itself on the observations, making it impossible to properly fit the sounding curves with synthetic data from layered models. In these cases, it is desirable that the inversion of one sounding be allowed to influence the inversion of its neighbouring soundings, in such way that the demand for fitting the data can be relaxed in favor of the demand to generate laterally smooth solutions.

The method described in this paper performs the joint inversion of data from a set of MT sounding stations, each one generating a sequence of resistivity values that represent a vertical column in a layered model. All columns, one for each measuring station have the same number of layers of the same thicknesses. The method applies lateral smoothing constraints between the resistivities in the same layers in the columns corresponding to adjacent sounding stations (Fig. 1).

.

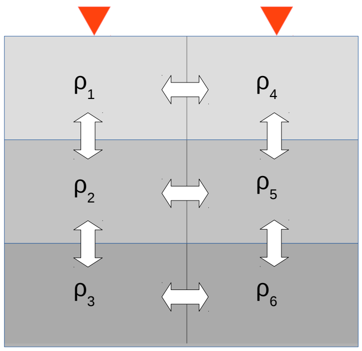

Figure 1: Example of the organization of parameters in a 2D structure. The red triangles represent sounding stations.

In all the examples shown here the method is applied to synthetic data from 2D transverse magnetic (TM) propagation mode surveys. The observed data are the real $Re(\hat{Z}_1)$ and imaginary $Im(\hat{Z}_1)$ components of the apparent impedance vector. The interpretive model is a horizontal plane-parallel layered medium and the parameters are the logarithmic values of the resistivities of each layer (Zhdanov, 2002; Santos, 2004).

Inversion theoretical revision

Most of the geophysical problems are non-linear, meaning that the observed data are not a linear combination of the model parameters. A geophysical dataset **d**, with N_o observations, is to be fit by synthetic data generated from the N_p model parameters in vector **P**. The relationship between the synthetic data $\mathbf{d}_s$ and the parameter set is in the form

$$\mathbf{d}_s = \mathbf{F}(\mathbf{P}), \tag{1}$$

where **F** is an non-linear vector function that represents the forward modeling operator. This vector function also depends on the frequency ω, and on the measurement position (x,y,z).

Since the function $\mathbf{F}$ doesn't have a unique inverse, the problem of determining a set of parameters that generate synthetic data that approximate the observations is defined as that of minimizing a functional ϕ_d that measures the misfit of the model's forward response **F**(**P**) for a given set of parameters **P** to the observed data **d**:

$$\phi_d(\mathbf{P}) = \|\mathbf{d}-\mathbf{F}(\mathbf{P})\|^2 = [\mathbf{d}-\mathbf{F}(\mathbf{P})]^T[\mathbf{d}-\mathbf{F}(\mathbf{P})] \tag{2}$$

In this study, the minimization of the nonlinear functional ϕ_d, with respect to **P**, was performed iteratively by the Gauss-Newton method with the Marquardt's modification (Marquardt, 1963) .

Regularized Inverse Problem

After the introduction of regularization, a function called objective function is created and the vector of parameters **P** that is to be found is obtained by minimizing this objective function ϕ_α, given by:

$$\phi_\alpha(\mathbf{P}) = \phi_d(\mathbf{P}) + \alpha\,\phi_{REG}(\mathbf{P}) \tag{3}$$

where α is a positive scalar called the regularization parameter that controls the importance of the information inserted by the regularizing functional.

Global Smoothness

The Global Smoothness or first-order Tikhonov (Tikhonov and Arsenin, 1977) regularization leads to solutions in which the differences between parameter values are minimal, that is, variations between parameter values are smooth. The mathematical representation of the functional ϕ_{GS} is:

$$\phi_{GS}(\mathbf{P}) = \|\mathbf{SP}\|_2^2 \tag{4}$$

S is a matrix which stores the relation between the parameters, each line being filled with 1 and -1 in the positions of the pairs of parameters to be related and zeros in the other positions.

Total Variation

The Total Variation regularizer also leads to stable solutions that are globally smooth, but it allows local discontinuities that clearly mark abrupt changes in the parameter values. The mathematical representation of the functional ϕ_{TV}, using an approximation proposed by Vogel (1997), is:

$$\phi_{TV}(\mathbf{P}) = \|\mathbf{SP}\|_1 \cong \sum_{k=1}^{N_d}[(P_i-P_j)_k^2+\beta]^{1/2} \tag{5}$$

where β is a small and positive scalar.

Gauss-Newton method with Marquardt's strategy

The objective function ϕ_α (Eq. 3) is treated as a second order approximation $\hat{\phi}_\alpha$ of ϕ_α around point $\mathbf{P}_k$, with the second order and higher derivatives equal to zero, since the non-linear geophysical functional is approximated by a linear function in **P**.

$$\hat{\phi}_\alpha(\mathbf{P}) \simeq \phi_\alpha(\mathbf{P}_k) + \Delta\mathbf{P}_k^t\mathbf{g}_k^\alpha + \frac{1}{2}\Delta\mathbf{P}_k^t\mathbf{H}_k^\alpha\Delta\mathbf{P} \tag{6}$$

where $\Delta\mathbf{P}_k$ is the perturbation vector of the parameters, in the k-th iteration, and

$$\mathbf{g}_k^\alpha = (\nabla_{\mathbf{P}}\phi_\alpha)\,|_{\mathbf{P}=\mathbf{P}_k} \tag{7}$$

$$\mathbf{H}_k^\alpha = (\nabla\nabla_{\mathbf{P}}^t\phi_\alpha)\,|_{\mathbf{P}=\mathbf{P}_k} \tag{8}$$

are, respectively, the gradient vector and the Hessian (second derivative matrix) of the functional ϕ_α, both with respect to the vector **P** avaliated in $\mathbf{P}_k$.

Then, the gradient vector of $\hat{\phi}_\alpha$ is calculated with respect to vector $\Delta\mathbf{P}_k$ and equated to the null vector. After some mathematical manipulations (Pujol, 2007), the updated parameter vector in the k-th iteration is:

$$\mathbf{P}_{k+1} = \mathbf{P}_k + (2\mathbf{A}^t\mathbf{A} + \alpha\,\mathbf{H}^{REG})^{-1}(2\mathbf{A}^t(\mathbf{d}-\mathbf{F}(\mathbf{P})) - \alpha\,\mathbf{g}^{REG}) \tag{9}$$

where **A** is the sensitivity matrix, defined as:

$$\mathbf{A}_{ij} = \frac{\partial\mathbf{F}_i(\mathbf{P})}{\partial\mathbf{P}_j}\,|_{\mathbf{P}=\mathbf{P}_k}\,. \tag{10}$$

$\mathbf{g}^{REG}$ and $\mathbf{H}^{REG}$ are the gradient vector and the Hessian of the regularizing functional.

Marquardt (1963) suggests adding a factor λ (Marquardt coefficient) to the diagonal of the Hessian matrix to stabilize the steps of the process. It is a positive scalar and its value is changed during the inversion process, according to the analysis of the objective function $\hat{\phi}_\alpha$, in a given estimate, with respect to the previous estimate. After the addition of the Marquardt parameter, Eq. 9 turns to:

$$\mathbf{P}_{k+1} = \mathbf{P}_k + (2\mathbf{A}^t\mathbf{A} + \alpha\mathbf{H}^{REG} + \lambda\mathbf{I})^{-1}(2\mathbf{A}^t(\mathbf{d} - \mathbf{F}(\mathbf{P})) - \alpha\mathbf{g}^R) \quad (11)$$

where $\mathbf{I}$ is the identity matrix.

Application

To illustrate the use of the inversion algorithm, we present its application to two different sets of synthetic data, generated by a 2D forward modelling finite element program, each one representing a specific geological structure. The synthetic data of each problem were contaminated with 2% Gaussian noise. The starting models for the examples presented here were a 200 Ohm-m homogeneous earth. The stability of the solution was tested by performing the inversion of the same data set contaminated with different random noise sequences.

Model 1

The first model (Fig. 2) represents a two-layer earth with a vertical fault. The data comprises ten equally spaced measuring stations, going from -5km to 5km, with 21 logarithmically spaced frequencies in the range of 0.1 Hz to 1000 Hz. Figure 3 shows the corresponding apparent resistivity pseudo section for model 1. Except for the position of the fault, this model represents a layered earth, with a 150 m thick layer to the left of the fault and a 300 m thick layer to the right. Therefore, most sounding stations record data that can be well fit by a 1D interpretive model. This example illustrates a situation in which one is better off using no lateral constraint. So, for this case each sounding was inverted independently, as a usual 1D inversion, using the GS and TV constraints in the vertical direction only. The inversion results using no lateral constraints are presented in Figure 4.

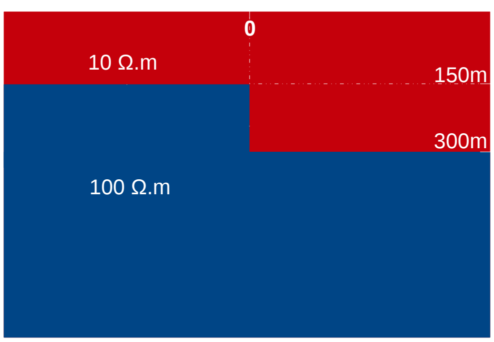

Figure 2: Section view of model 1.

The independent 1D inversion of each sounding yields an approximation of the original model geometry. It can be noted that there is no big difference between the results using the GS and VT regularizations, except for the more oscillatory nature of the GS solution, which in this case is observed in the variations of the resistivities in each column. The resistivities of each layer are estimated to a good approximation, throughout the grid except in the column closest to the position of the fault. Moreover, the fault itself is clearly resolved.

Because the model is predominantly 1D, that is, with no big lateral variations of resistivity, the independent 1D inversion of each sounding is good enough to determine the layer interfaces and its resistivities.

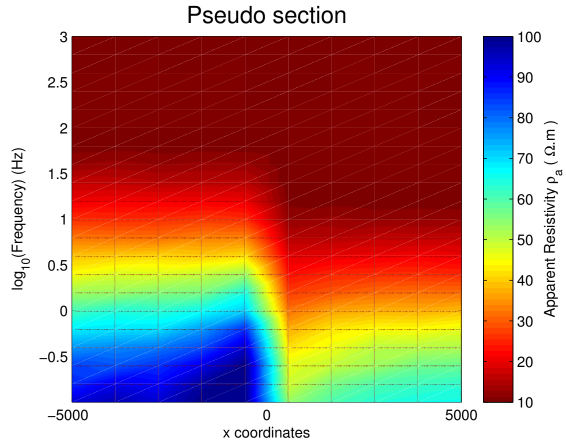

Figure 3: TM mode apparent resistivity pseudo section from model 1.

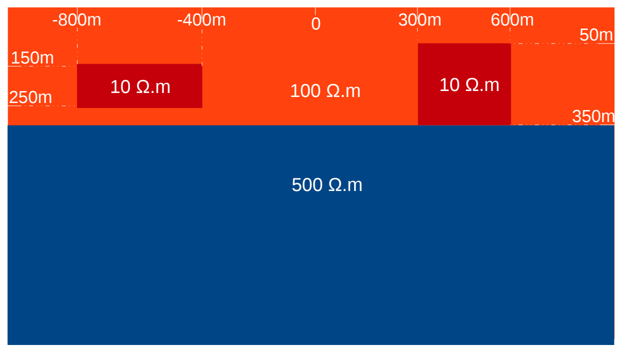

Figure 5: Section view of the model 2.

Model 2

Figures 5 and 6 show the second model tested in this study and its corresponding apparent resistivity pseudo section. This is a two-layer model containing two conductive bodies (10 ohm.m) located in the upper layer. The data comprises 15 equally spaced measuring stations, going from -1km to 1km, with 21 logarithmically spaced frequencies, varying from 0.1Hz to 1000Hz.

The inversion results using the GS and TV regularizations in the vertical direction only (no lateral constraints), are presented in Figure 7.

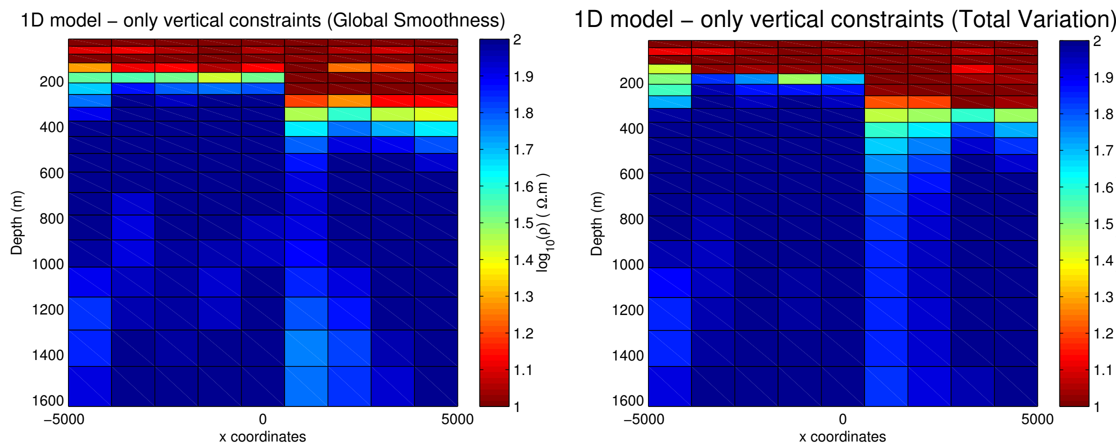

Figure 4: Resistivity models obtained by 1D inversion using (a) Global Smoothness and (b) Total Variation regularization in the vertical direction and no lateral constraints.

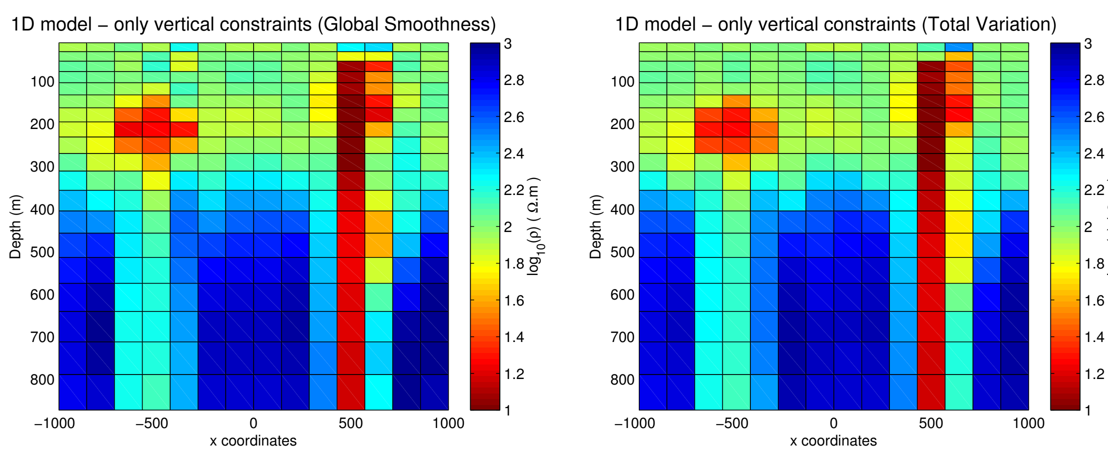

Figure 7: Resistivity models obtained by 1D inversion using (a) GS and (b) TV regularizations in the vertical direction and no lateral constraints.

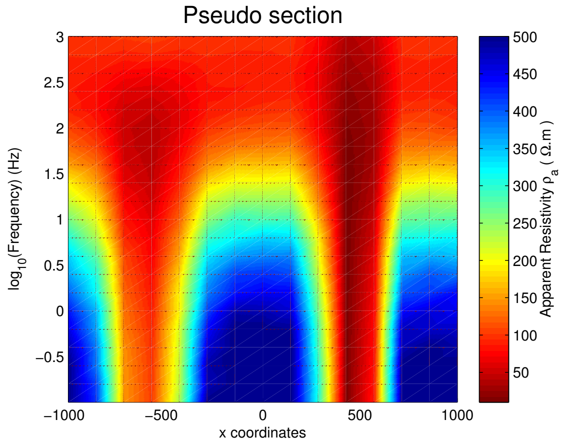

Figure 6: Pseudo section.

The vertical constraint creates an unwanted smoothing, with a smudged area below the location of each block. This shaded area is even bigger below the second block, probably because its base coincides with the horizontal interface. For this case, the independent 1D inversion of each sounding can not give a good solution, because now there's no station which isn't under the influence of the 2D structures.

The laterally constrained inversion (LCI) of the synthetic data generated by model 2 resulted in the resistivity models shown in Figure 8.

Both Figures show good results in the sense of detecting the presence of the two conductive bodies and the position of the interface between the layers. The effect of the vertical constraint, that spread the influence of the conductive bodies down through the columns, is now balanced by the influence of the lateral constraints, so the bodies are better delineated using the LCI.

The inversion result using the GS regularization is somewhat "over smoothned". This is most noticeable is the positions below the conductive blocks, where the artifacts created by the vertical constraints are stronger. Because of that, the definition of the interface is impaired.

The inversion with the TV constraints was more efficient in delineating the bodies both horizontally and vertically, despite the permanence of the vertical constraint effect.

The apparent resistivity and phase curves are used to show the data fitting in Figures 9 and 10, with the GS and TV regularizations, respectively. Note that in this case the data can not be as well fit as in the first case (model 1), because now there's really no measuring station on a position far from the 2D structures.

CONCLUSION

The results show that the 1D laterally constrained inversion method applied to MT data is an effective way for delineating 2D geoelectrical structures. It generates very fast results in detecting 2D isolated structures, resulting in an efficient and inexpensive tool for quick imaging, especially on areas which can not be well approximated by layered models.

Compared to results using only vertical constraints, where the soudings are inverted independently, the LCI decreases the smeared area created by the vertical constraint below 2D structures. The results using LCI could also be used as interpretive (initial) models of a 2D inversion algorithm, avoiding solutions that correspond to local minima.

ACKNOWLEDGMENTS

This research is partly funded by PETROBRAS, through project number 0050.0088121.13.9–UFPA/FADESP/PETROBRAS, as part of the Research Network of Applied Geophysics. Régis is recipient of the CNPq research grant.

References

Auken, E., and A. V. Christiansen, 2004, Layered and laterally constrained 2d inversion of resistivity data: Geophysics, **69**, no. 3.

Auken, E., A. V. Christiansen, B. H. Jacobsen, N. Foged, and K. I. Sorensen, 2005, Piecewise 1d laterally constrained inversion of resistivity data: Geophysical Prospecting, **53**.

Constable, S. C., R. L. Parker, and C. G. Constable, 1987, Occam's inversion: A practical algorithm for generating smooth models from electromagnetic sounding data: The Leading Edge, **52**, no. 3.

Hadamard, J., 1902, Sur les problèmes aux dérivées partielles et leur signification physique: Princeton University Bulletin, **13**, 49–52.

Marquardt, D. W., 1963, An algorithm for least-squares estimation of non-linear parameters: J. of the Society for Industrial and Applied Mathematics, **11**, 431–441.

Martins, C. M., W. A. Lima, V. C. Barbosa, and J. ao B. Silva, 2011, Total variation regularization for depth-to-basement estimate: Part 1 - mathematical details and applications: Geophysics, **76**, I1–I12.

Miorelli, F., 2011, Joint laterally constrained inversion of csem and mt data: Presented at the 73rd EAGE Conference & Exhibition incorporating SPE EUROPEC 2011.

Pujol, J., 2007, The solution of nonlinear inverse problems and the Levenberg-Marquardt method: Geophysics, **72**, W1.

Santos, F. A. M., 2004, 1d laterally constrained inversion of em34 profiling data: Journal of Applied Geophysics, **56**, no. 2.

Tikhonov, A. N., and V. Y. Arsenin, 1977, Solutions of ill-posed problems: New York: Winston.

Vogel, C. R., 1997, Nonsmooth regularization: Rundell (Eds.), Inverse Problems in Geophysical Applications, 1–11.

Vozoff, K., 2012, *in* 8. The Magnetotelluric Method: 641–712.

Zhdanov, M. S., 2002, Geophysical inverse theory and regularization problems, 1 ed.: Elsevier Science. Methods in geochemistry and geophysics 36.

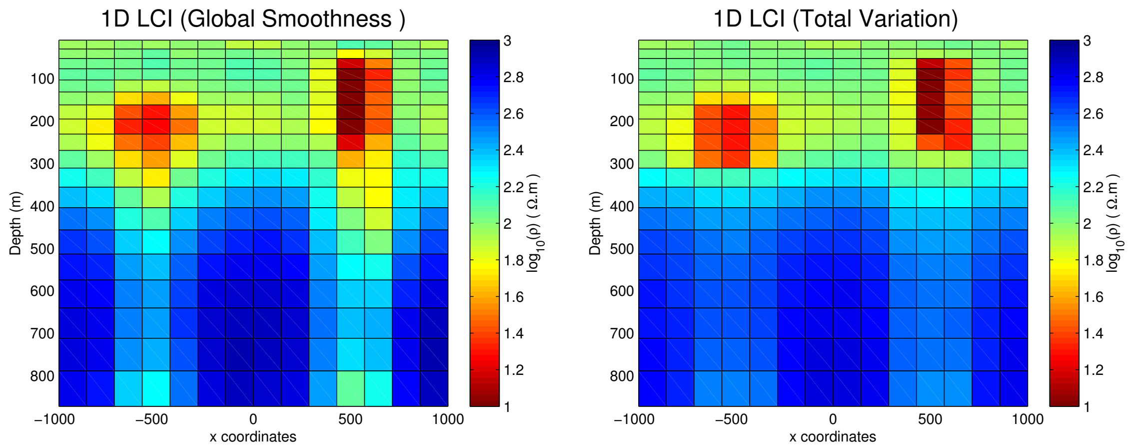

Figure 8: Resistivity models obtained by 1D LCI using (a) GS ($\lambda = 10^4$ and $\alpha = 10^{-4}$) and (b) TV ($\lambda = 10^4, \alpha = 3 \times 10^{-4}$ and $\beta = 10^{-2}$) regularizations in both vertical and lateral directions.

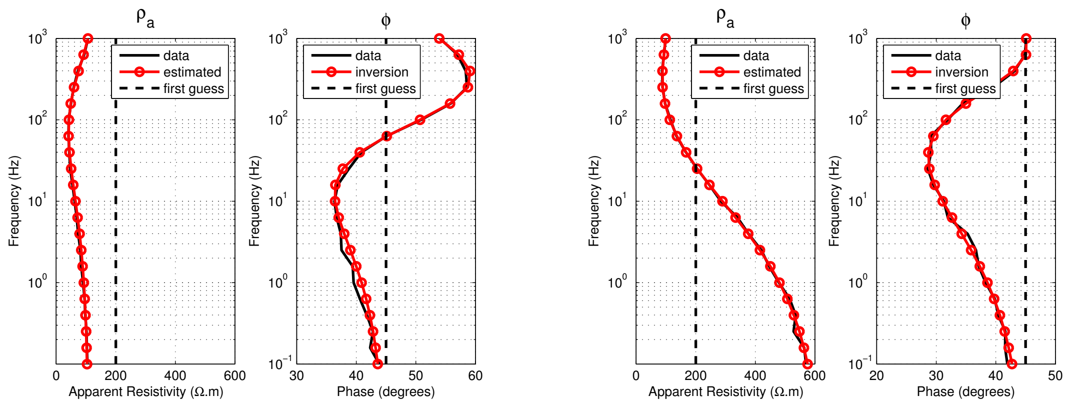

Figure 9: Data adjustment curves for positions (a) $x \simeq -0.57km$ above the first block (b) $x \simeq 0.001km$ right in the middle of the two blocks.

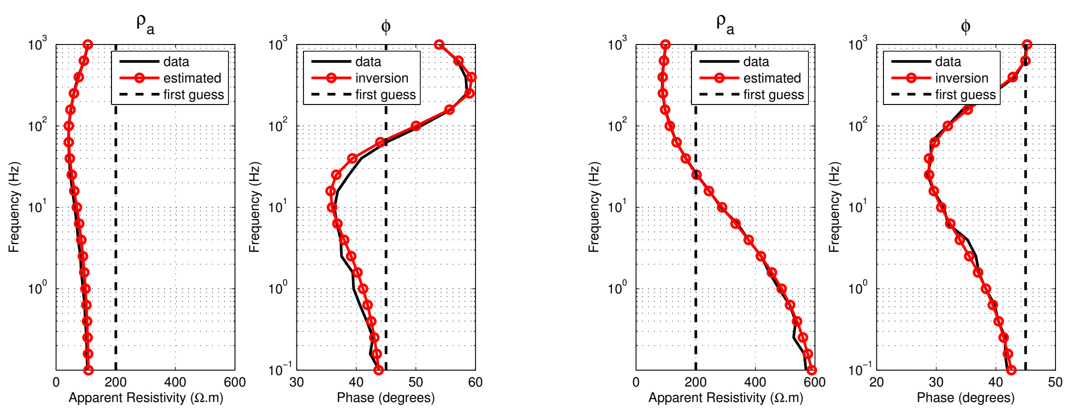

Figure 10: Data adjustment curves for positions (a) $x \simeq -0.57km$ above the first block and (b) $x \simeq 0.001km$ right in the middle of the two blocks.